Graphene-Based Metal Oxide Nanocomposites for Gas Sensing Application

Naveen Kumar J. R.[1, 2], Shrinivasa Mayya D.[2], Savitha M. B.[3], & Prasad P.*[1, 2]

[1]Department of Nano Technology, Srinivas Institute of Technology, Mangaluru, Karnataka – 574143, INDIA

[2]Srinivas Centre for Nano Science and Technology, Srinivas University, Mangaluru, Karnataka – 574146, INDIA

[3]Department of Chemistry and Research Centre, Sahyadri College of Engineering and Management, Sahyadri Campus, Adyar, Mangaluru, Karnataka - 575007, INDIA

*E-mail: hodnanotechsit@gmail.com

+

Type of the Paper: Research Paper.
Type of Review: Peer Reviewed.
Indexed In: OpenAIRE.
DOI: http://doi.org/10.5281/zenodo.1481293.
Google Scholar Citation: IJAEML

How to Cite this Paper:
Naveen Kumar, J. R., Shrinivasa Mayya, D., Savitha, M. B., & Prasad, P. (2018). Graphene-Based Metal Oxide Nanocomposites for Gas Sensing Application. *International Journal of Applied Engineering and Management Letters (IJAEML)*, *2*(2), 98-115.
DOI: http://doi.org/10.5281/zenodo.1481293.

International Journal of Applied Engineering and Management Letters (IJAEML)
A Refereed International Journal of Srinivas University, India.

Graphene-Based Metal Oxide Nanocomposites for Gas Sensing Application

Naveen Kumar J. R.[1,2], Shrinivasa Mayya D.[2], Savitha M. B.[3], & Prasad P.*[1,2]

[1]Department of Nano Technology, Srinivas Institute of Technology, Mangaluru, Karnataka – 574143, INDIA

[2]Srinivas Centre for Nano Science and Technology, Srinivas University, Mangaluru, Karnataka – 574146, INDIA

[3]Department of Chemistry and Research Centre, Sahyadri College of Engineering and Management, Sahyadri Campus, Adyar, Mangaluru, Karnataka - 575007, INDIA

*E-mail: hodnanotechsit@gmail.com

ABSTRACT

Recently, graphene-based materials have engaged the attentiveness of all researchers doing research related to materials science, particularly related to gas sensing application. Graphene nanocomposites or nanohybrids are the modern inclusion to the marvel applications of graphene-based materials. One of the occupying utilisation of the graphene-based nanocomposites is chemical detection which is beneficial for observing the explosive nature, harmfulness and inflammability of gases. Diversified metal oxides like tin oxide, ferric oxide, zinc oxide and indium oxide as soon as combined with graphene-based materials to form nanocomposites own enormous potentiality for detecting a minute amount of harmful gas. In this article, the various synthesising methods, preparation of composites, fabrication and gas sensing utilisation of graphene-based nanocomposites are depicted in detail.

Keywords: Metal oxides, graphene oxide, reduced graphene oxide, nanocomposites, gas sensor.

1. INTRODUCTION :

There is a growing state of affairs on metal oxide semiconducting gas sensors in beyond a long time regarding the view of human health and environmental protection. Many nanostructured metallic oxides with the high surface to volume region have appreciably investigated like sensing substances [1–5]. Between them, ordered mesoporous metal oxides hold enormous interest since their available pores advantage over diffusion of gas molecules for growing response rate, but additionally the reduction in aggregation and sintering for enhancing their thermal stability under immoderate temperature throughout the fabrication and operating procedure of gas sensor [6–12]. Tiemann and co-workers [13] perceived the increased sensitivity of mesoporous indium oxide for methane. Mao et al. [14]. Moreover, stated a tremendous sensitivity regarding hierarchically mesoporous hematite microsphere towards formaldehyde. Lai et al. [15] introduced a cost-effective synthesis of mesoporous indium oxide with tunable pore wall thickness with the aid of without delay using solvent-extracted mesoporous silica together with exclusive pore sizes as a template. The gas-sensing character over those mesoporous semiconducting metal oxide sensors could remain in extension enhance further thru doping noble metals.

Tu et al. [16] observed that Pt-doped mesoporous indium oxide own an extensively superior response than those besides doping Pt. Lai et al. [17] suggested the greater suitable gasoline-sensing character on silver-doped mesoporous indium oxide towards formaldehyde. Even though, the growing cost resulted from noble metals may control their practical application. Detection of ammonia (NH_3) within the atmosphere is of significant importance to environmental protection also from the chemical and automotive industries [18]. Surveys taken by the U.S. activity safety and health administration

showed that exposure to NH_3, of that concentration surpassing 50 ppm, could cause temporary vision defect and irritations to human bodies [19]. Several works had been done regarding NH_3 sensors, and ancient metal oxides supported most of them. However, the bulk of metal compound primarily based sensors will solely operate at elevated temperatures (more than 200˚C) [20, 21]. To comprehend the detection of NH_3 at temperature, individuals have done numerous works and studied a range of sensitive materials [22–31]. Novel carbon materials like carbon nanotube and graphene are established to be ideal sensing materials to construct superior gas sensors, which will work at room temperature [32, 33].

Graphene has been considered as a promising candidate for building electrically based gas sensors since its electronic properties can be strongly affected by the absorption and desorption of the gas molecules, which is attributed to high quality of crystal lattice leading to a quite low electronic noise and the two-dimensional structure providing great sensing area per unit volume [55].

SnO_2, a useful n-type semiconductor material, is reported according to stay sensitive to many gases including reductive gases (e.g., acetone, hydrogen, ethanol, methanol) or poisonous gases (e.g., NO_2, H_2S), consequently is broadly used in commercial gas sensors [34-36]. Owing by the unique properties regarding SnO_2 nanoparticles such as no toxicity, small dimension, low cost, and high theoretical capacity, the SnO_2 gas sensor has been extensively studied and attracted large interest [37, 38]. However, gas sensor based of pure SnO_2 nanoparticles suffers mean sensitivity and long response recovery time [39, 40], because SnO_2 nanoparticles tend imitation of total easily, as hampers the diffusion over gas molecules on the surface of the semiconductor. For SnO_2 nanomaterials, that is known up to anticipate particle size, specific surface area; then equal dispersion radically influence the gas sensing overall performance [41, 42]. Specifically, small sized, widespread surface area and well-dispersed nanoparticles can easily adsorb gasoline molecules and enhance the gas sensing properties [43, 44].

Graphene and graphene-related materials are mostly conductors or insulators [45]. So, an uphill task of the graphene research community is to produce semiconducting graphene material for sensor and other electronic applications [46]. There has been substantial progress in this direction and doping of graphene by metal ions has been successfully achieved. However, the major contribution has been achieved through chemical modifications of graphene molecules, mostly by composite formation [47]. Graphene-metal oxide hybrid composite (GMO) is one such example [48, 49] for electrical and electrochemical applications including sensors.

Among the transition metal oxides, haematite (α-Fe_2O_3), the foremost stable iron oxide part underneath ambient conditions with bandgap (Eg) of 2.1 eV, is especially engaging for gas sensors, catalysis, lithium-ion batteries, optical devices, and pigments owing to its high chemical stableness, mean cost, harmlessness, and high immunity to corrosion [50-54]. For gas-sensing Huang et al. [55] produced synthetical porous α-Fe_2O_3 nanoparticles by natural annealing of β-FeOOH base material derived from a flexible hydrothermal method for superior H_2S identification. Tan et al. [56] with success created a network of porous α-Fe_2O_3 micro-rods that exhibited a higher response, ultra-fast response–recovery, and superior long stability than compact α-Fe_2O_3 nanoparticles. The nanoscale α-Fe_2O_3 porous structure demonstrates high response worth, fast response, and sensible property compared with mesoporous α-Fe_2O_3 [57].

Nanoporous hematite nanoparticles show higher sensitivities than compact α-Fe_2O_3 nanoparticles as a result of the former's standard structure [58]. The α-Fe_2O_3 gas sensors prepared from Fe_3O_4-chitosan with porous surface present a much superior response to hydrogen, carbon monoxide, ethanol, and ammonia compared with the device prepared from pure iron oxide [59]. Figure 1 shows potential applications areas of graphene. In this work, we are focusing on review of reduced graphene and metal oxide based nanocomposites, synthesising methods, fabrication process and sensing response related to gas sensing application.

2. SYNTHESIS OF GRAPHENE-BASED NANOCOMPOSITES :

2.1 Synthesis of ZnO-RGO based nanocomposites

Tao Wanga et al. [60] produced ZnO nanowires in a bulker way by a modified carbothermal reduction technique that was reported by Z.H. Zhou et al. [61]. Typically, 1.0 g ZnO powder and 1.0

g graphite (500 mesh) were mixed and relocated into a quartz tube oven. Then the oven was heated to 1150˚C in an environment of N_2 (4.5 L/min) and air (0.1 L/min) as a carrier gas and reactive gas, severally. Once concerning five minutes, the product was administrated by the carrier gas and around 0.8 g ZnO nanowires yield can be obtained. Schematical flow diagram for the mass production of ZnO nanowires by modified carbothermal reduction technique is as shown Figure 2.

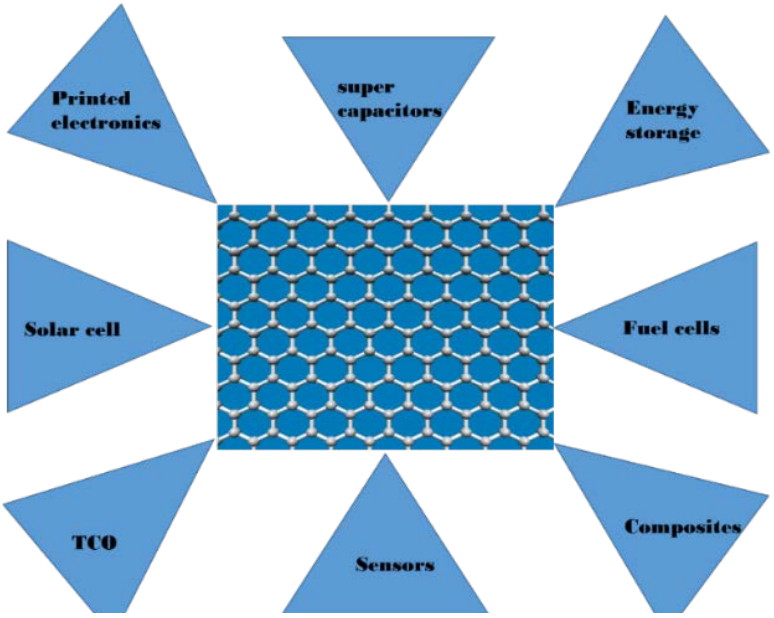

Fig. 1: Potential applications of graphene

Modified Hummers method was a well-established technique for graphene oxide synthesis [62]. The standard process was as follows, graphite (1 g) and conc. H_2SO_4 (25 mL) were combined in a 250 mL of the flask, and vigorous stirring was executed. Also, 1.25 g of $NaNO_3$ was transferred to the reaction mixture. After keeping stirring for 1 h, the mixture was chilled to 0˚C using an ice-water bath. 3.7 g of $KMnO_4$ was transferred in little portions during 2 hrs, accompanied by advancing the temperature to 35˚C and allowed to react for 2 hrs. Later on, the reaction was quenched by adding 100 mL of drinking water 6 and 3.5 mL of hydrogen peroxide (30%). The consequent graphene oxide was filtered, and wash out with lots of aqueous hydrogen chloride (3%) till no precipitation of barium sulfate occurred in the influence of aqueous barium chloride solution. Additional wash out with water was carried out till the chloride test with silver nitrate was negative, and also the consequent products were dried at 40˚C for 24 hr in the vacuum oven. Figure 3 shows schematic flow diagram for the synthesis of GO by modified Hummer's method.

The method for synthesizing ZnO nanowire-rGO nanocomposites is illustrated in Figure 4. during a distinctive process, 0.5 g GO was dispersed in D.I. water by the assistance of ultra-sonication to make the GO solution, then a certain quantity of ZnO nanowires and 0.1 g PVP were dispersed in D.I. water with ultrasonic for an additional 15 min. later on, 2 solutions were mixed and stirred for 1 h, accompany by centrifuging and wash out with deionized water for many times to separate impurities. At last, the nanocomposites were dried in an oven long and thermally reduced at 300˚C for concerning five min underneath the protection of Ar to make ZnO NW-RGO nanocomposites.

The method for synthesizing ZnO nanowire-rGO nanocomposites is illustrated in Figure 4. during a distinctive process, 0.5 g GO was dispersed in D.I. water by the assistance of ultra-sonication to make the GO solution, then a certain quantity of ZnO nanowires and 0.1 g PVP were dispersed in D.I. water with ultrasonic for an additional 15 min. Later on, 2 solutions were mixed and stirred for 1 h, accompany by centrifuging and wash out with deionized water for many times to separate impurities. At last, the nanocomposites were dried in an oven long and thermally reduced at 300˚C for concerning five min underneath the protection of Ar to make ZnO NW-RGO nanocomposites.

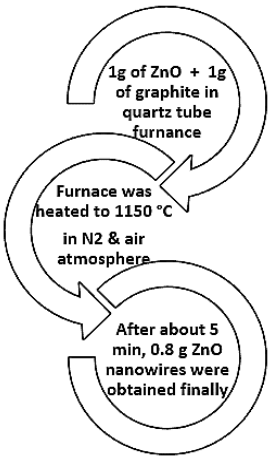

Fig. 2: Schematical flow diagram for the mass production of ZnO nanowires by modified carbothermal reduction technique

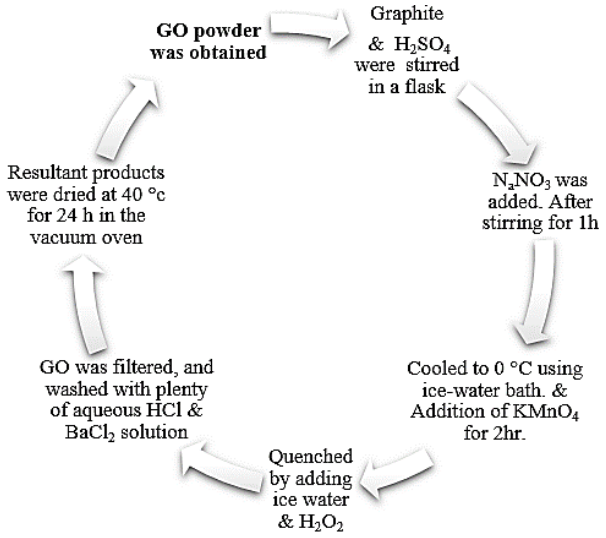

Fig. 3: Schematic flow diagram for the synthesis of graphene oxide by modified Hummer's method

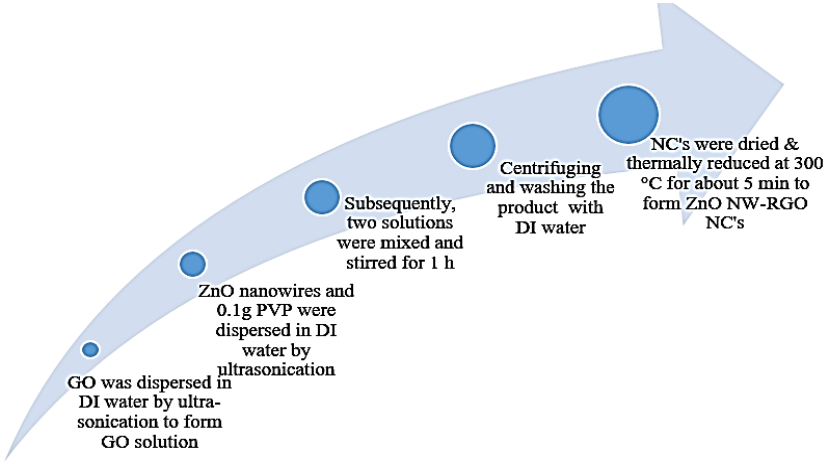

Fig. 4: Schematic flow diagram for synthesizing ZnO NW-RGO nanocomposites

2.2 Synthesis of SnO_2-rGO based nanocomposites

GO can be prepared through a modified Hummers approach [63]. Where concentrated sulphuric acid (300 mL) then $NaNO_3$ (4 g) had been mixed along with graphite powder (5 g) in an ice-bath tub under

stirring all-night. Then, $KMnO_4$ (25 g) was carefully added in accordance with the reaction mixture beneath stirring for 24 hrs till the solution become pink to brown. After that, the solution used to be added in accordance with D.I. water (500 mL) and heated at 90˚C till it becomes golden yellow. The receiver solution was once percolated and washes out with hydrogen chloride or D.I. water a number of times, individually. As-prepared graphene oxide used to be achieved and dissolved in D.I. water for utilization. Figure 5 shows schematic flow diagram for the synthesis of GO by modified hummer's approach.

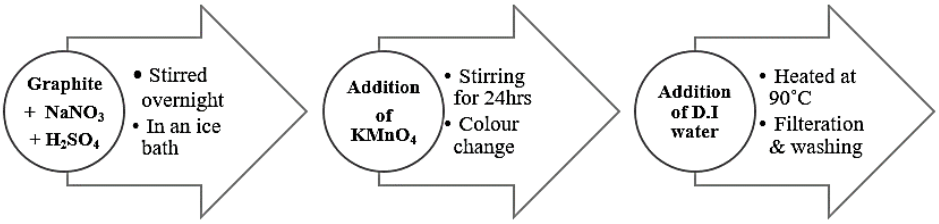

Fig. 5: Schematic flow diagram for synthesis of GO by modified hummer's approach

Through a normal synthesis procedure, $SnCl_2$ ethylene glycol (EG) solution was formed. Then $SnCl_2{\cdot}2H_2O$ (3 g) used to be dissolved in EG (200 mL). GO (13.2 mg) was once dissolved among EG (200 mL) and deionized water (10 mL), together with ultrasonic treatment for 30 minutes, which was slowly added according to the above formed $SnCl_2$-EG solution. Afterward, the mixture used to be heated at 140˚C for 2 hrs. After cooling down to atmospheric temperature, the precipitate used to be washed out together with D.I. water and ethanol various times and dried underneath vacuum at 80˚C overnight. Finally, SnO_2-rGO powders were obtained. Pure SnO_2 can be prepared by means of the above technique but without GO. Schematic flow diagram for the synthesis of SnO_2-rGO composite is shown in Figure 6.

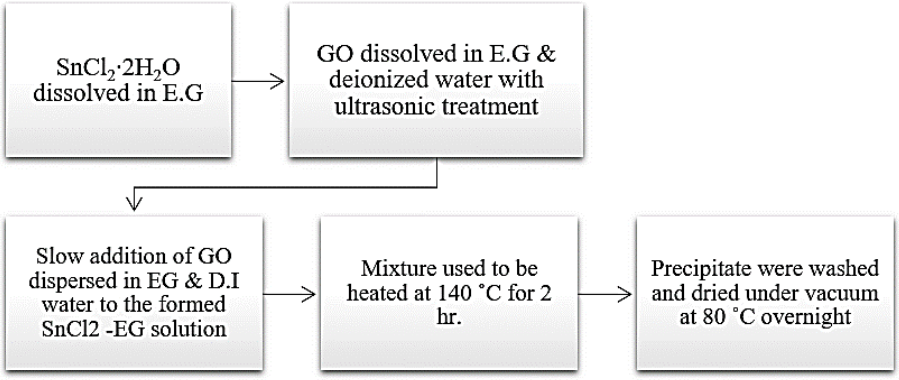

Fig. 6: Schematic flow diagram for synthesis of SnO_2-rGO composite

2.3 Synthesis of ordered mesoporous In_2O_3 nanoparticle-rGO based nanocomposites

Using hydrothermal method ordered silica kit-6 can be synthesized at 130˚C of hydrothermal temperature in accordance with well-known process [64]; wherein 0.6 g of kit-6 became dispersed inside 10 mL of ethanol, accompanied with the aid of addition of 1.2 g of hydrated $In(NO_3)_3$ underneath stirring in a beaker. After all the solvent had evaporated from the beaker, the resulting powder used to be treated with heat in a ceramic crucible at 250 ˚C for 3 hrs in an oven, in order to decompose indium nitrate. Sooner or later, the silica template used to be eliminated at room temperature using 2 mol/L sodium hydroxide. The stable product turned into recovered by centrifugation, determined thru wash out with water several instances after which drying at 70˚C overnight.

Figure 7 shows schematic float diagram for the synthesis of ordered mesoporous In_2O_3 nanoparticles. Go used to be synthesized by the Hummers' modified method [65, 66]. A two gram of natural graphite powder and 1.5 g of sodium nitrate had been placed in a beaker. Then 46 mL of

conc. sulphuric acid was brought slowly with stirred in an ice bath setup.
A seven gram of potassium permanganate powder was added carefully with constant stirring, then the mixture used to be stirred for 2 hrs. after which heated at 35˚C for 2 hrs., perceived through adding step by step a hundred mL of D.I. water. The mixture was heated at ninety-degree Celsius for 30 min and then delivered steadily 200 mL of D.I. water. When the temperature reduces to 60˚C, 30 mL of hydrogen peroxide (5 wt %) was added. The combination becomes centrifuged and wash out with hundred mL over hydrogen chloride (5 wt %) and 900 mL of D.I. water.
A 1 g approximately graphite oxide was added to the beaker followed by dispersing GO in 1000 mL of deionized water under ultra-sonication for 30 min. The reaction mixture used to be centrifuged at a pace of 1,000 r min^{-1}, followed via discarding the solid then the ultrasonic process has to be repeated thrice. Graphene oxide was collected from the reaction mixture by way of centrifugation approximately around 15,000 r min^{-1} speed for 30 minutes, followed by drying in a chamber for seventy-two hour; around 0.2 g graphene oxide used to be dispersed amongst 2 hundred mL of D.I. water, followed thru including 0.25 g of hydrazine solution (eighty wt%). The pH of suspension has to be maintained at 10 by adding conc. NH_3 solution (2.4 mL). The aggregate was heated underneath stirring at 90˚C for three hours and cooled to room temperature. RGO was collected by centrifugation at a pace of 15,000 r min^{-1} for 30 min. Later dried at room temperature for 72 hrs. Figure 8 shows schematic glide diagram for synthesis graphene oxide and its reduced form.

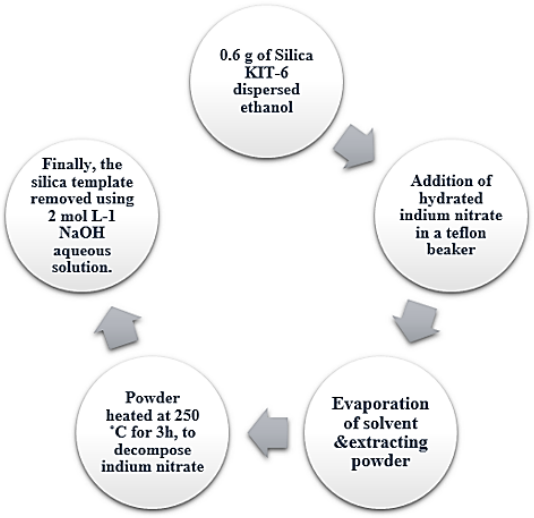

Fig. 7: Schematic flow diagram for synthesis of ordered mesoporous In_2O_3 nanoparticle

Synthesis of the ordered mesoporous In_2O_3 nanoparticle-rGO nanocomposites schematic diagram is as shown in Figure 9. Where 0.2 g of ordered mesoporous In_2O_3 nanoparticle dispensed in 5 mL of D.I. water, accompanied by adding 0.05 wt% of reduced GO water suspension relative to the quantity of ordered mesoporous In_2O_3 nanoparticles distributed within the reaction mixture. The blended solution was ultrasonicated for fifteen min, and consequently, the solid composite becomes collected by the filter and dried at 70˚C all night.

2.4 Synthesis of Fe_3O_4-rGO based nanocomposites

Graphene oxide can be synthesized from inexpensive graphite powder using well-known Hummers modified methodology [67] that was thought of as a straightforward and efficient chemical methodology with a high yield as compared with different routes like chemical vapor deposition, micro-mechanical exfoliation of extremely ordered pyrolytic graphite and epitaxial growth [68].

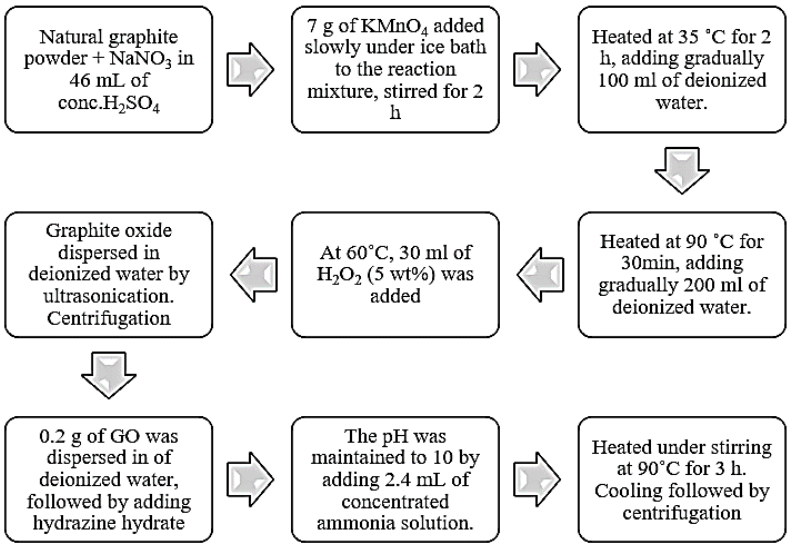

Fig. 8: Schematic flow diagram for the synthesis of graphene oxide and its reduction.

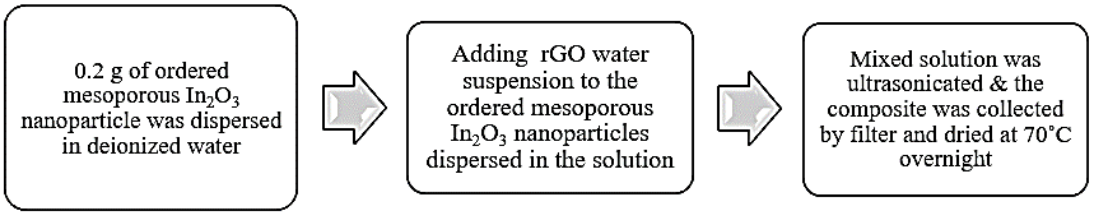

Fig. 9: Schematic flow diagram for Synthesis of ordered mesoporous In_2O_3 nanoparticle-rGO nanocomposites

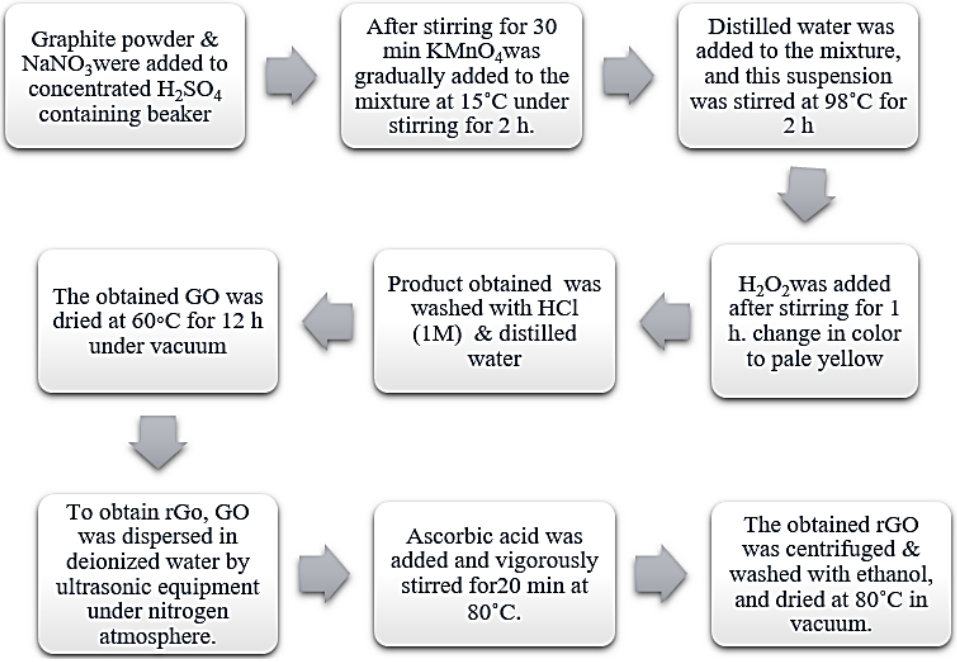

Fig. 10: Schematic flow diagram for synthesis of graphene oxide and its reduction

For GO synthesis, 1 g of graphite powder and 0.5 g of sodium nitrate were value added to 23 mL of conc. sulphuric acid (95%) under continuous stirring for 30 min. Once the graphite powder was well distributed, 3 g of potassium permanganate was added bit by bit to the reaction mixture at

15˚C under stirring for 2 hr. Then, 46 ml of D.I. water was poured into the reaction mixture, and this suspension was stirred constantly at 98˚C for 2 hr. Finally, 7 mL of H_2O_2 was slowly added with stirring for 1h as the reaction progressed, the color of the mixture modified to bright yellow. The collected powder was washed with HCl (1 M) aqueous solution to get rid of metal ions followed by distilled water to get rid of the acid. The obtained GO was dried at 60˚C for 12 hrs. underneath vacuum. To get rGO, 0.1 g of the as-synthesized graphene oxide was suspended in 100 ml of D.I water by ultrasonic equipment for 1 h under nitrogen atmosphere. About 0.15 g of ascorbic acid was added and continuously stirred for 20 min at 80˚C. The obtained rGO was centrifuged, washed with ethyl alcohol, and dried at 80˚C in vacuum condition. Figure 10 shows schematical flow diagram for the synthesis of graphene oxide and its reduction to get reduced graphene oxide.

The Fe_3O_4/rGO nanocomposites can be prepared by a hydrothermal route [69]. In a very typical synthesis, 0.025 g of rGO suspended in 50 mL of H_2O through ultrasonic treatment for 1 h underneath inert N_2 atmosphere. The pH of rGO suspension (11–12) was adjusted by ammonium solution (25 wt. %). afterward, 0.05 g of $FeCl_2$ was added to the rGO solution and vigorously stirred for 16 hrs. at atmospheric temperature. The obtained Fe_3O_4/rGO was recovered, washed with water and ethyl alcohol many terms, and dehydrated in a vacuum at 80˚C for 5 hr. The as-prepared Fe_3O_4/rGO was heated at a continuing rate of 2˚C min−1 in the air to 600˚C and maintained at this temperature for 5h to get α-Fe_2O_3 porous network. Figure 11 shows schematic flow diagram for the synthesis of the α-Fe_2O_3 porous network from Fe_3O_4 - rGO composite.

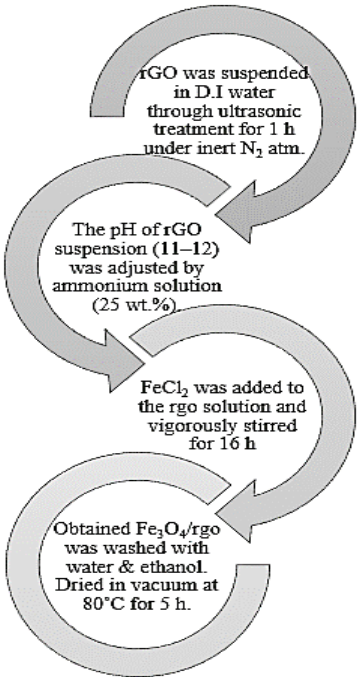

Fig. 11: Schematic flow diagram for synthesis of α-Fe_2O_3 porous network from Fe_3O_4 - rGO composite

3. GAS SENSING AND DEVICE FABRICATION MECHANISM :

3.1 Gas sensing and device fabrication of ZnO-rGO based nanocomposites mechanism

A homespun/homemade gas sensing element testing system can be built and used to generate NH_3 and monitor resistance changes of the sensors [62, 70-74]. N_2 can be used because the carrier gas and N_2/O_2 (80/20) both will be used as the diluting and background gas. N_2 was purged into the NH_3 solution and also the carried NH_3 was bubbled out over a dry tube full of sodium hydroxide flakes to obtain the dry NH_3 gas. Analytic gas with completely different concentrations will be obtained by combining the saturated vapors with the diluting gas in a gas mixer. The obtained mixed gas should

purge passing through a gas device placed within the gas chamber that connected to the testing device [60]. Agilent 4156C device can be used to check the resistance variation of the device, that will modify once exposed to the analytic gas.

3. 2. Mechanism of gas sensing and device fabrication for SnO_2-rGO based nanocomposites

Electrochemical sensor checking out can conduct over a sensor platform Yanhong Chang et al. [75]. Briefly, 5 mg SnO_2-rGO composites have been combined with a little drop of D.I. water to form a paste. The prepared paste can be coated as like a layer over the outer surface of the ceramic rod and dried in air. After that, the ceramic pipe coated including the as-prepared paste heated at 400˚C in a nitrogen atmosphere for 2 hrs. Finally, the gas sensor can be applied to the detecting system. Figure 12 shows schematic flow diagram for Gas Sensing and Device Fabrication for SnO_2-rGO based nanocomposites.

Fig. 12: Schematic flow diagram for Gas Sensing and Device Fabrication for SnO_2-rGO based nanocomposites.

3.3 In_2O_3-rGO based nanocomposites gas sensing mechanism and device fabrication

Sensors can made-up with the aid of dip-coating the samples on a ceramic tube with 2 Au electrodes and four platinum wire, according to the method [3, 5]. The powder samples had been 1st dispersed in water, forming a suspension. The suspension becomes coated onto the external surface of the ceramic tube to attach the 2 Au electrodes, and additionally, the sensing element became dried at a temperature to densify the sensing film. The electrical response of the gasoline sensor can be measured with a WS-60A device Ping Xue et al. [76].

3. 4 Mechanism of gas sensing and device fabrication for Fe_3O_4-rGO based nanocomposites

The synthesized α-Fe_2O_3 porous network can spread ethyl alcohol by ultrasonication. A suspension drop containing α-Fe_2O_3porous network will be dropped on the Pt-interdigitated electrodes made-up on a SiO_2/Si substrate employing a micropipette then gradually dried at temperature. The sensors could be heat-treated at 600˚C for five h to stabilize resistance. The gas sensing character of haematite porous nanostructures were studied and correlated by examining all the sensors with ethanol (10–ppm), carbon monoxide (10–200 ppm) hydrogen (25–1000 ppm), and ammonia (50–1000 ppm) at totally distinct temperatures (350˚C–450˚C) employing a homemade assemble with elevated speed switch gas flow. Nguyen Thi Anh Thua et al. [77]. The system utilizes a continuing rate of two hundred sccm throughout sensing measure; the resistance of the sensors can be automatically documented using Keithley 2602.

4. METAL OXIDE-GRAPHENE BASED NANOCOMPOSITES SENSOR RESPONSE :

4.1. ZnO-RGO based nanocomposites sensor response

Tao Wanga et al. [60] worked together to get the most effective quality ratio of ZnO nanowires and RGO for NH_3 detection, they took 5 samples using ZnO nanowires content intercalated RGO for the experiment, with the ZnO content of 0%, 10%, 25%, 50% and 100%, respectively. Pure ZnO nanowires have been proved not appropriate for building a gas sensor since the device cannot recover to the initial state. Compared with the 25 Wt% ZnO-RGO primarily based device, the 10 wt% ZnO-RGO primarily based sensor shows a faster response to NH_3, however the variation of the sensor resistance reaches solely concerning 6%, that is why lower and the recovery time is also for much longer compared with the 25 wt% ZnO-RGO sample. The 50 wt% ZnO-RGO exhibits a similar response worth to NH_3 compared with 25 wt% ZnO-RGO, however, once NH_3 is turned off, the resistance of the sensor cannot return to the initial worth, namely, the sensor cannot get over the

reaction. Above all, the most effective content of ZnO nanowires is 25 wt%. The combination of ZnO and RGO can form homogeneous heterojunction, which can promote the transfer of electrons and reduce the activation energy required for ammonia to react on the surface of the sensitive material. As a result, the sensor shows excellent properties of ammonia detection.

Influencing factor in the ZnO-RGO based nanocomposites is because of resistance changes, reason is that after thermal annealing, Fermi level moves downwards away from the Dirac point, resulted in the lowered Fermi level thus the conductivity enhances [60]. The other reason is that when the annealing temperature gets higher, the contacts between graphene and ZnO nanowires become better and the surfactant remaining on the surface of the material is removed, leading to better electron transfer between two materials.

4. 2 Gas-sensing properties on the SnO_2-rGO composites

Yanhong Chang et al. [75] fabricated a gas sensor based on SnO_2-rGO composites then pure SnO_2under the identical pilot conditions were investigated. The gas sensors had been examined for gases including different mean concentrations 0.56 x 10^{-6}, 1.12 x 10^{-6} or 1.68 x 10^{-6} or the gas sensing testing temperature used to be 300˚C. At the attention over 1.12 x 10^{-6}, the sensitivities of ethanol then H_2S are 22 and 11, respectively, exhibits strong performance of SnO_2-rGO gasoline sensor. However, the sensitivities regarding SnO_2 gas sensor are 15 and 7, respectively. Obviously, the composites have greater sensitivity than luminous SnO_2 for each ethanol yet H_2S. SnO_2-rGO has quick explanation excerpt time. For example, for ethanol on 1.12 x 10^{-6}, the response and excerpt day over SnO_2-rGO is solely 5 and 9 s, respectively. However, it was determined so much tidy SnO_2 gas sensor is no longer absolutely touchy yet its response then recovery duration is 22 then 36 s, respectively. Besides, the stability concerning the gasoline sensor primarily based on SnO_2-rGO used to be additionally examined. The sensing properties were investigated because of a hebdomad by means of consistently introducing the ethanol yet H_2S along the equal concentrations. The significant decrease in gasoline sensing attribute used to be no longer observed, indicating the good over SnO_2-rGO gas sensor. As a result, in the presence of rGO, the gas sensing properties have been greatly improved. It reveals that rGO plays a crucial role in the gas sensing system. Therefore, the as-prepared composites would be a novel highly efficient sensing material in the outstanding feature gas sensing application. Due to the excellent physicochemical properties of rGO sheets, the gas sensor will yield good sensing performance.

4. 3 Gas-sensing properties on the In_2O_3 -rGO based nanocomposites

Ping Xue et al. [76] did studies on mesoporous In_2O_3-reduced graphene oxide nanocomposite is employed as gasoline sensing substances and fabricated into the gas device for investigation its gas-sensing ability. The natural mesoporous In_2O_3 nanoparticles are referred to assessment. The reaction of the gasoline sensor fabricated from mesoporous In_2O_3-reduced graphene oxide nanocomposite to one hundred ppm ethanol in the air became examined as performing of operative temperature; this is relatively low at under 230˚C. It reaches a maximum well worth at regarding three hundred degree Celsius then step by step decreases if greater increasing the operational temperature, the gasoline-sensing mechanism of the gas tool is mainly supported a conduction modification deriving from the assimilation of oxygen at the surface of sensing materials and the response between pre-adsorbed element species and ethanol. As soon as the device is located in air, the pre-absorbed detail molecules may also capture electrons from the conductivity band of In_2O_3 and remodel into chemisorbed element species (O^{2-}, O^- and O^{2-}), ensuring a lower in electron concentration and conductivity. As soon as ethanol is brought, it will react with the oxygen species and additionally, the captured electron can be injected back to the conductivity band, resulting in a rise in electron concentration and conduction. Once the operative temperature will increase, the pre-absorbed element molecules might also capture additional electrons [5, 78, 79], consequently resulting in a better reaction. Though, chemisorbed element species might have a tendency to drop from the surface of sensing materials as temperature increases, results in the downfall of response. The top-quality in operation temperature should be determined with the aid of the balance of these 2 strategies [80]. Consequently, the choicest operational temperature for the mesoporous In_2O_3-reduced graphene oxide nanocomposite-primarily based apparatus turned into 300˚C.

The reaction to ethanol will boom quickly with the growing of gas absorption. The correlation among

the reaction and ethanol attention is just about linear in the range of 100–1,000 ppm, that indicates that those sensors region unit terribly appropriate for the recognition of ethanol throughout a broad choice. Unsaturation development to comparatively high ethanol absorption is also derived from the huge particular vicinity and sizable pore quantity of mesoporous In_2O_3 imparting a number of surface energetic sites and accommodating a massively wide variety of ethanol gas molecules. They also look at what the device fabricated from ordered mesoporous In_2O_3-reduced graphene oxide nanocomposite exhibited a reaction to ethanol over the entire examining out attention vary stronger than that of mesoporous In_2O_3 and additionally the response of the previous to at least one thousand ppm ethanol gasoline is sort of 23 instances above that of the concluding (2,778 and 119 respectively), that still possesses big advantages of the reaction towards ethanol even in comparison with one-of-a-kind In_2O_3-based totally sensing substances in accordance [81–87]. The reaction improvement is likewise defined by the exhibits the most critical response to plant product amongst all of the examine gases. Furthermore, the advent of rGO failed to extensively increase the reaction time (ninety-seven and ninety-eight s for the sensors supported mesoporous In_2O_3 and mesoporous indium oxide - reduced graphene oxide nanocomposite in the direction of 1,000 ppm ethanol) and inversely lessen the restoration time (sixty and thirty one's for such 2 sensors respectively). All the previous outcomes suggest that the device supported mesoporous In_2O_3-rGO nanocomposite is probably helpful for sensing ethanol.

Here influencing parameter is operating temperature as operating temperature increases; the pre-absorbed oxygen molecules could capture more electrons thus result in a higher response.

4.4 Gas-sensing properties on the Fe_2O_3-rGO based nanocomposites

Nguyen Thi Anh Thua et al. [77] worked on the α-Fe_2O_3 nanoporous network for gas sensing application, they have tested the fabricated device to different gases, as well as CO (10–200 ppm), H_2 (25–1000 ppm), and NH_3 (50–1000ppm). The obtained response to completely different CO gas concentrations at 350˚C, 400˚C, and 450˚C showed that the α-Fe_2O_3 nanoporous network was comparatively sensitive to CO gas [77]. Responses of the current sensors lightly varied at the working temperature vary from 350˚C–450˚C. The optimum operating temperature was also 400˚C that concurred with the results of the C_2H_5OH gas tests. The testing results with completely different CO gas concentrations additionally revealed that the sensor responses to10–200 ppm solely slightly increased at all operating temperatures. At the optimum temperature (400˚C), the response values to 100 and 200 ppm CO gas were approximately 1.8 and 1.9, respectively. The ∝-Fe_2O_3 porous network additionally exhibited low sensitivities to H_2 and NH_3 gases. The response values of ∝-Fe_2O_3 porous network-based sensors to H_2 gas (25–1000 ppm) and NH_3 gas (50–1000 ppm) solely slightly increased from 1.2 to 1.9 respectively. Advantageous property to focus on gas is one of the crucial aspects of gas sensors. Response standards of Fe_2O_3 porous network-based sensors to C_2H_5OH, CO, H_2, and NH_3 were 9.5, 1.8, 1.5, and 1.1, respectively, indicating that the sensors presented good selectivity to C_2H_5OH. The response times were fast enough for practical applications but the recovery times were relatively long. This problem should be improved by several techniques such as UV radiation or pulsed heating at high temperatures. Therefore, the Fe_2O_3porous net-work is highly promising for use in high-quality sensor materials for alcohol breath analyzers [77].

Sensing properties also influenced by intrinsic porous structures originating from the oxidation of rGO, which could generate more active sizes and improve the gas diffusion coefficient. Future directions in graphene based metaloxide nanocomposites should have focus on new materials and the mechanism that governs the sensing performance. As new processing and fabrication techniques become available and allow designing complex structures. Several ways of enhancing the response, sensitivity and selectivity in nanostructured metal oxide based heterojunction materials by engineering of the potential energy barrier at the interface by using a second constituent, introduction of selective p-n and n-p-n response inversions.

5. CONCLUSIONS & FUTURE OUTLOOK :

In conclusion, ZnO nanowire-reduced graphene oxide based nanocomposites can be prepared by a simple approach, wherever each ZnO nanowires and GO can be produced in large scales. On comparing with RGO or ZnO nanowire-based sensors, the ZnO NW-RGO based NH_3 sensors

demonstrate glorious overall sensing performance with the greater response, shorter response, recovery time, good selectivity, and sensible stability. In addition, the sensor contains a very small size and low power consumption that is crucial for system integration and transportable equipment. The achievements of the sensors based on ZnO NW-RGO nanocomposites with exceptional performance are likely to supply a universal platform for the detection of harmful gases in the future. SnO_2-rGO based nanocomposites found that SnO_2 grew evenly on the surface on rGO layers. The introduction of rGO could prevent the agglomeration concerning SnO_2 nanoparticles. The study related to SnO_2-rGO gas sensor had higher sensitivities and shorter responding period in contrast to coherent SnO_2, demonstrating an environment-friendly gas sensor based over SnO_2-graphene. In_2O_3-rGO based nanocomposites thru a combining hard templet and ultrasonic mixing method. The ensuing mesoporous In_2O_3 nanoparticle-rGO nanocomposite exhibited a considerable high response to ethanol as compared to those absolute mesoporous In_2O_3 while not rGO, that suggests the ability use of such unique nanostructured material for recognition ethanol gas. An analogous method is probably prolonged to different mesoporous metallic oxide–rGO nanocomposite gasoline materials with definitely exceptional compositions, pore structure, and volume. The evaluation would possibly open up new possibilities for preparing superior substances based on various ordered mesoporous metallic oxide–rGO nanocomposite for multipurpose applications. Synthesis of Fe_3O_4-rGO based composite can be done by simple approach. The gas-sensing characteristics indicated that the α-Fe_2O_3 porous network exhibited sensible sensitivity, outstanding selectivity, and high stability as an ethanol sensor.

REFERENCES :

[1] Batra, A. K., Chilvery, A. K., Guggilla, P., Aggarwal, M., & Currie, J. R. (2014). Micro- and Nano-Structured Metal Oxides Based Chemical Sensors: An Overview. Journal of Nanoscience and Nanotechnology, 14(2), 2065–2085. https://doi.org/10.1166/jnn.2014.9266

[2] Wang, G. L., Lai, X. Y., & Wang, D. (2013). Synthesis and Characterization of Hollow Cadmium Oxide Sphere with Carbon Microsphere as Template. Journal of Nanoscience and Nanotechnology, 13(2), 1423–1426. https://doi.org/10.1166/jnn.2013.5960

[3] Lai, X., Li, J., Korgel, B. A., Dong, Z., Li, Z., Su, F., Wang, D. (2011). General synthesis and gas-sensing properties of multiple-shell metal oxide hollow microspheres. Angewandte Chemie-International Edition, 50(12), 2738–2741. https://doi.org/10.1002/anie.201004900

[4] Yu, R., Li, Z., Wang, D., Lai, X., Xing, C., Yang, M., & Xing, X. (2010). Fe2TiO5/??-Fe_2O_3 nanocomposite hollow spheres with enhanced gas-sensing properties. Scripta Materialia, 63(2), 155–158. https://doi.org/10.1016/j.scriptamat.2010.03.043

[5] Zhenmin, L., Xiaoyong, L., Hong, W., Dan, M., Chaojian, X., & Dan, W. (2009). General synthesis of homogeneous hollow core-shell ferrite microspheres. Journal of Physical Chemistry C, 113(7), 2792–2797. https://doi.org/10.1021/jp8094787

[6] Tiemann, M. (2007). Porous metal oxides as gas sensors. Chemistry A European Journal, 13(30), 8376–8388. https://doi.org/10.1002/chem.200700927

[7] Lai XY, Shen GX, Xue P. (2015). Ordered mesoporous NiO with thin pore walls and its enhanced sensing performance for formaldehyde. Nanoscale, 7, 4005–4012.

[8] Zhao JJ, Zheng MB, Lai XY. (2012). Preparation of mesoporous In_2O_3 nanorods via a hydrothermal-annealing method and their gas sensing properties. Mater. Lett., 75, 126–129.

[9] Lai XY, Wang H, Mao D. (2008). Mesoporous indium oxide synthesized via a nanocasting route. Mater. Lett., 62, 3868–3871.

[10] Sun XH, Hu XD, Wang YC. (2015). Enhanced gas-sensing performance of Fe-doped ordered mesoporous NiO with long-range periodicity. J. Phys. Chem. C, 119, 3228–3237.

[11] Sun XH, Hao HR, Ji HM. (2014). Nanocasting synthesis of In_2O_3 with appropriate mesostructured ordering and enhanced gas-sensing property. ACS Appl. Mater Interfaces 6, 401–409.

[12] Gao Q, Zheng WT, Wei CD. (2013). Methanol-sensing property improvement of mesostructured zinc oxide prepared by the nanocasting strategy. J. Nanomater. 2013, 263852.

[13] Wagner T, Kohl CD, Morandi S. (2012). Photo-reduction of mesoporous In_2O_3: mechanistic model and utility in gas sensing. Chem. Eur. J., 18, 8216–8223.

[14] Mao D, Yao JX, Lai XY. (2011). Hierarchically mesoporous hematite microspheres and their enhanced formaldehyde-sensing properties. Small, 7, 578–582.

[15] Lai XY, Wang D, Han N. (2010). Ordered arrays of bead chain- like In_2O_3 nanorods and their enhanced sensing performance for formaldehyde. Chem. Mater., 22, 3033–3042.

[16] Tu JC, Li N, Lai XY. (2010). H_2S-sensing properties of Pt-doped mesoporous indium oxide. Appl. Surf. Sci., 256, 5051–5055.

[17] Lai XY, Li P, Yang TL. (2012). Ordered an array of Ag–In_2O_3 composite nanorods with enhanced gas-sensing properties. Scr. Mater., 67, 293–296.

[18] Timmer, B., Olthuis, W., Van den Berg, A. (2005). Ammonia sensors and their applications - a review. Sens. Actuator. B, 107, 666–677.

[19] Zaman, M. S., Moon, C. H., Haberer, E. D. (2014). Sensitive ammonia gas sensors fabricated using biologically assembled copper sulfide. Appl. Phys. Express, 7, 117002.

[20] Ryu, S. R., Ram, S. D. G., Cho, H.-d., Lee, D. J., Kang, T.W., Woo, Y. (2015). Single ZnO nano cactus gas sensor formed by etching of ZnO nanorods. Nanoscale, 7, 11115–11122.

[21] Yu, N., Zhang, H., Davidson, S. D., Sun, J. M., Wang, Y. (2016). Effect of ZnO facet on ethanol steam reforming over Co/ZnO. Catal. Commun., 73, 93–97.

[22] Setkus, A., Galdikas, A., Mironas, A., Simkiene, I., Ancutiene, I., Janickis, V. (2001). Properties of Cu_xS thin film based structures: influence on the sensitivity to ammonia at room temperatures. Thin Solid Films, 391, 275–281.

[23] Sagade, A. A., Sharma, R. (2008). Copper sulfide (Cu_xS) as an ammonia gas sensor working at room temperature. Sens. Actuator. B, 133, 135–143.

[24] Rao, G. S. T., Rao, D. T. (1999). The Gas sensitivity of ZnO based thick film sensor to NH_3 at room temperature. Sens. Actuator. B, 55, 166–169.

[25] Du, N., Zhang, H., Chen, B., Ma, X., Liu, Z., Wu, J. (2007). Porous indium oxide nanotubes: Layer-by-layer assembly on carbon-nanotube templates and application for room-temperature NH_3 gas sensors. Adv. Mater., 19, 1641–1645.

[26] Zhu, G., Zhang, Q., Xie, G., Su, Y., Zhao, K., Du, H. (2016). Gas sensors based on polyaniline/zinc oxide hybrid film for ammonia detection at room temperature. Chem. Phys. Lett., 665, 147–152.

[27] Sharma, A., Bhojane, P., Rana, A. K., Kumar, Y., Shirage, P. M. (2017). Mesoporous nickel cobalt hydroxide/oxide as an excellent room temperature ammonia sensor. Scripta. Mater., 128, 65-68.

[28] Nie, Q., Pang, Z., Lu, H., Cai, Y., Wei, Q. (2016). Ammonia gas sensors based on In_2O_3/PANI heteronanofibers operating at room temperature. Beilstein. J. Nanotech., 7, 1312–1321.

[29] Liu, Y., Wang, L., Wang, H., Xiong, M., Yang, T., Zakharova, G. S. (2016). Highly sensitive and selective ammonia gas sensors based on PBS quantum dots/TiO_2 nanotube arrays at room temperature. Sens. Actuator. B, 236, 529–536.

[30] Li, Z., Lin, Z., Wang, N., Wang, J., Liu, W., Sun, K. (2016). High precision NH_3 sensing using network nano-sheet Co_3O_4 arrays based sensor at room temperature. Sens. Actuator. B, 235, 222–231.

[31] Kulandaisamy, A. J., Reddy, J. R., Srinivasan, P., Babu, K. J., Mani, G. K., Shankar, P. (2016). Room temperature ammonia sensing properties of ZnO thin films grown by spray pyrolysis: Effect of Mg doping. J. Alloys Compd., 688, 422–429.

[32] Cui, S., Pu, H., Lu, G., Wen, Z., Mattson, E. C., Hirschmugl, C. (2012). Fast and selective room temperature ammonia sensors using silver nanocrystal-functionalized carbon nanotubes. ACS Appl. Mater. Inter., 4, 4898–4904.

[33] Wang, T., Huang, D., Yang, Z., Xu, S. S., He, G. L., Li, X. L. (2016). A review on graphene-based gas/vapor sensors with unique properties and potential applications. Nano-Micro Lett., 8, 1–25.

[34] Williams, G., Coles, G. S. V. (1993). NOx response of tin dioxide based gas sensors. Sens. Actuator B-Chem., 15-16, 349-353.

[35] Wang, Q., Zhang, L.S., Wu, J. F. (2010). J. Phys. Chem. C, 114, 22671-22676.

[36] Patil, S. B., Patil, P. P., More, M. A. (2007). Acetone Vapour Sensing Characteristics of Cobalt-doped SnO_2 Thin Films. Sens. Actuator B-Chem., 125, 126-130.

[37] Zhang, B., Russell, J. M., Shi, W. S. (2004). Large-Scale, solution-phase growth of single-crystalline SnO_2 nanorods. J. Am. Chem. Soc., 126, 5972-5974.

[38] Zhang, D. F., Sun, L. D., Li, C. J. (2005). Hierarchical assembly of SnO_2 nanorods arrays on α – Fe_2O_3 nanotubes: a case of interfacial lattice compatibility. J. Am. Chem. Soc., 127, 13492-13493.

[39] Justin, T., Mccue, J., Wang, Y. (2007). SnO_2−In_2O_3 Nanocomposites as Semiconductor Gas Sensors for CO and NOx Detection. Chem. Mater., 19, 1009-1015.

[40] Zhang, Y. H., He, Y. Q. (2007). Front. Mater. Sci. China, 1, 297-303.

[41] Li, L. L., Zhang, W. M., Yuan, Q., Li, Z. X., Fang, C. J. (2008). Room temperature ionic liquids assisted green synthesis of nanocrystalline porous SnO_2 and their gas sensor behaviours. Cryst. Growth Des., 8, 4165-4172.

[42] Liu, Y., Koep, E., Liu, M. L. (2005). A Highly Sensitive and Fast-Responding SnO_2 Sensor Fabricated by Combustion Chemical Vapor Deposition. Chem. Mater., 17, 3997-4000.

[43] Kim, H. R., Choi, K. I., Lee, J. H., Akbar, S. A. (2009). Highly sensitive and ultra-fast responding gas sensors using self-assembled hierarchical SnO_2 spheres. Sens. Actuator B-Chem., 136, 138-143.

[44] Firooza, A. A., Mahjouba, A. R., Khodadadib, A. A. (2009). Highly sensitive CO and ethanol nanoflower-like SnO_2 ensor among various morphologies obtained by using single and mixed ionic surfactant templates. Sens. Actuator B Chem., 141, 89-96.

[45] Anasori, B., Beidaghi, M., & Gogotsi, Y. (2014). Graphene-Transition metal oxide hybrid materials. Materials Today. Elsevier. https://doi.org/10.1016/j.mattod.2014.04.043

[46] Sun, M., Liu, H., Liu, Y., Qu, J., Li, J. (2015). Graphene-based transition metal oxide nanocomposites for the oxygen reduction reaction. Nanoscale, 7, 1250–1269.

[47] Zhang, W., Liu, F., Li, Q., Shou, Q., Cheng, J., Zhang, L., Nelson, B. J., Zhang, X. (2012). Transition metal oxide and graphene nanocomposites for high-performance electrochemical capacitors. Phys. Chem. Chem. Phys., 14, 16331–16337.

[48] Khan, M., Tahir, M. N., Adil, S. F., Khan, H. U., Siddiqui, M. R. H., Al-warthan, A. A., Tremel, W. (2015). Graphene based metal and metal oxide nanocomposites: Synthesis, properties and their applications. J. Mater. Chem. A, 3, 18753–18808.

[49] Hu, C., Lu, T., Chen, F., Zhang, R. (2013). A brief review of graphene–metal oxide composites synthesis and applications in Photocatalysis. J. Chin. Adv. Mater. Soc., 1, 21–39.

[50] Kaneti, Y. V., Zakaria, Q. M. D., Zhang, Z., Chen, C., Yue, J., Liu, M., Jiang, X., Yu, A. (2014). solvothermal synthesis of ZnO-decorated-Fe_2O_3 nanorods with highly enhanced gas-sensing performance toward n-butanol. J. Mater. Chem. A, 2, 13283, http://dx.doi.org/10.1039/C4TA01837K.

[51] Zhang, S., Zhang, P., Xie, A., Li, S., Huang, F., Shen, Y. (2016). A Novel 2D porous print fabric-like-Fe_2O_3 sheet with high performance as the anode material for lithium-ion battery. Electrochim. Acta, 212, 912–920.

[52] Wang, Y., Wang, S., Zhang, H., Gao, X., Yang, J., Wang, L. (2014). Brookite TiO_2 decorated-Fe_2O_3 nanoheterostructures with rod morphologies for gas sensor application. J. Mater. Chem. A, 2, 7935, http://dx.doi.org/10.1039/c4ta00163j.

[53] Jia, X., Yue, F., Chen, X., Pan H. -B., Liu, W. -G., Liu J. -Y. (2014). One-pot controlled the synthesis of single-crystal -Fe_2O_3 hollow nanostructure and its gas sensing properties. RSC Adv., 4, 42899–42904, http://dx.doi.org/10.1039/C4RA07275H.

[54] Wang, S., Wang, Y., Zhang, H., Gao, X., Yang, J., Wang, Y. (2014). Fabrication of porous-Fe_2O_3 nanoshuttles and their application for toluene sensors. RSC Adv., 4, 30840, http://dx.doi.org/10.1039/C4RA03743J.

[55] Huang, Y., Chen, W., Zhang, S., Kuang, Z., Ao, D., Alkurd, N. R. (2015). A high-performance hydrogen sulfide gas sensor based on porous-Fe_2O_3 operates at room-temperature. Appl. Surf. Sci., 351, 1025–1033. http://dx.doi.org/10.1016/j.apsusc.2015.06.053.

[56] Tan, J., Chen, J., Liu, K., Huang, X. (2016). Synthesis of porous -Fe_2O_3microrods via in situ decompositions of FeC_2O_4 precursor for ultra-fast responding and recovering ethanol gas sensor. Sens. Actuators B, 230, 46–53, http://dx.doi.org/10.1016/j.snb.2016.02.012.

[57] Sun, X., Ji, H., Li, X., Cai, S., Zheng, C. (2014). Open-system nanocasting synthesis of nanoscale-Fe_2O_3 porous structure with enhanced acetone-sensing properties. J. Alloys Compd., 600, 111–117. http://dx.doi.org/10.1016/j.jallcom.2014.02.129.

[58] Cuong, N. D., Hoa, T. T., Khieu, D. Q., Hoa, N. D., Van Hieu, N. (2012). Gas sensor based on nanoporous hematite nanoparticles: effect of synthesis pathways on morphology and gas sensing properties. Curr. Appl. Phys., 12, 1355–1360. http://dx.doi.org/10.1016/j.cap.2012.03.026.

[59] Cuong, N. D., Hoa, T. T., Khieu, D. Q., Lam, T. D., Hoa, N. D., Van Hieu, N. (2012). Synthesis, characterization, and comparative gas-sensing properties of Fe_2O_3 prepared from Fe_3O_4 and Fe_3O_4-chitosan. J. Alloys Compd., 523, 120–126. http://dx.doi.org/10.1016/j.jallcom.2012.01.117.

[60] Tao Wanga, Zhen Suna, Da Huanga, ZhiYang,b, Qian Jia, Nantao Hua, Guilin Ying, Dannong Heb, Hao Weia, Yafei Zhang. (2017). Studies on NH_3 gas sensing by zinc oxide nanowire-reduced graphene oxide nanocomposites. http://dx.doi.org/doi:10.1016/j.snb.2017.05.162.

[61] Zhou, Z. H., Zhan, C. H., Wang, Y. Y., Su, Y. J., Yang, Z., Zhang, Y. F. (2011). Rapid mass production of ZnO nanowires by a modified carbothermal reduction method. Mater. Lett., 65, 832–835.

[62] Hu, N., Wang, Y., Chai, J., Gao, R., Yang, Z., Kong, E. S. -W. (2012). Gas sensor based on phenylenediamine reduced graphene oxide. Sens. Actuator. B, 163, 107–114.

[63] Gilje, S., Han, S., Wang, M., Wang, K. L., Kaner, R. B. (2007). Nano. Lett., 7, 3394-3398.

[64] Kleitz, F., Choi, S. H., Ryoo, R. (2003). Cubic Ia_3d large mesoporous silica: synthesis and replication of platinum nanowires, carbon nanorods, and carbon nanotubes. Chem Commun , 17, 2136–2137.

[65] Hummers WS, Offeman RE. (1958). Preparation of graphitic oxide. J. Am. Chem. Soc. 80, 1339-1406.

[66] Becerril HA, Mao J., Liu Z. (2008). Evaluation of solution-processed reduced graphene oxide films as transparent conductors. ACS Nano, 2, 463–470.

[67] Hummers, W. S., Offeman, R. E. (1958). Preparation of graphitic oxide. J. Am. Chem. Soc., 80, 1339. http://dx.doi.org/10.1021/ja01539a017.

[68] Pei, S., Cheng, H. (2012). The reduction of graphene oxide. Carbon, 50, 3210–3228. http://dx.doi.org/10.1016/j.carbon.2011.11.010.

[69] Teo, P. S., Lim, H. N., Huang, N. M., Chia, C. H., Harrison, I. (2012). Room temperature in situ chemical synthesis of Fe_3O_4/graphene. Ceram. Int., 38, 6411–6416. http://dx.doi.org/10.1016/j.ceramint.2012.05.014.

[70] Hu, N., Wang, Y., Chai, J., Gao, R., Yang, Z., Kong, E. S. W. (2012). Gas sensor based on phenylenediamine reduced graphene oxide. Sens. Actuator. B, 163, 107–114.

[71] Wang, Y. Y., Zhou, Z. H., Yang, Z., Chen, X. H., Xu, D., Zhang, Y. F. (2009). Gas sensors based on deposited Single-walled carbon nanotube networks for DMMP detection. Nanotechnology, 20, 345502.

[72] Shi, D., Wei, L., Wang, J., Zhao, J., Chen, C., Xu, D. (2013). Solid organic acid tetra fluoro hydroquinone functionalized single-walled carbon nanotube chemiresistive sensors for highly sensitive and selective formaldehyde detection. Sens. Actuator. B, 177, 370–375.

[73] Wei, L., Lu, D., Wang, J., Wei, H., Zhao, J., Geng, H. (2014). Highly sensitive detection of trinitrotoluene in water by the chemiresistive sensor based on noncovalently amino functionalized single-walled carbon nanotube. Sens. Actuator. B, 190, 529–534.

[74] Huang, D., Yang, Z., Li, X., Zhang, L., Hu, J., Su, Y. (2017), Three-dimensional conductive networks based on stacked SiO_2@graphene frameworks for enhanced gas sensing. Nanoscale, 9, 109–118.

[75] Yanhong Chang, Yunfeng Yao, Bin Wang, Hui Luo, Tianyi Li, Linjie Zhi. (2013). Reduced Graphene Oxide-Mediated SnO_2 Nanocrystals for Enhanced Gas-sensing Properties. J. Mater. Sci. Technol., 29(2), 157-160.

[76] Ping Xue, Xiaomei Yang, Xiaoyong Lai, Weitao Xia, Peng Li, Junzhuo Fang. (2015). Controlling synthesis and gas-sensing properties of ordered mesoporous In_2O_3-reduced graphene oxide (rGO) nanocomposite. https://doi.org/10.1007/s11434-015-0852-6.

[77] Nguyen Thi Anh Thu, Nguyen Duc Cuong, Le Cao Nguyen, Dinh Quang Khieu, Pham Cam Nam, Nguyen Van Toan, Chu Manh Hung, Nguyen Van Hieue. (2018). Fe_2O_3 nanoporous network fabricated from Fe_3O_4/reduced graphene oxide for high-performance ethanol gas sensor. https://doi.org/10.1016/j.snb.2017.09.154

[78] Kumazawa, N., Islam MR, Takeuchi, M. (1999). Photoresponse of a titanium dioxide chemical sensor. J Electroanal. Chem., 472, 137–141.

[79] Chu XF, Jiang DL, Zheng CM. (2007). The preparation and gas-sensing properties of $NiFe_2O_4$ nanocubes and nanorods. Sens. Actuators B Chem., 123, 793–797.

[80] Chang, J., Kuo, H., Leu, I. (2002). The effects of thickness and operation temperature on ZnO: Al thin film CO gas sensor. Sens. Actuators. B Chem., 84, 258–264.

[81] Li BX, Xie, Y., Jing, M. (2006). In_2O_3 hollow microspheres: a synthesis from designed $In(OH)_3$ precursors and applications in gas sensors and photocatalysis. Langmuir, 22, 9380–9385.

[82] Zhang, T., Gu, F., Han, D., Wang, Z., Guo, G. (2013). Synthesis, characterization and alcohol-sensing properties of rare earth doped In_2O_3 hollow spheres. Sensors and Actuators, B: Chemical, 177, 1180–1188. https://doi.org/10.1016/j.snb.2012.12.024

[83] Li, E., Cheng, Z., Xu, J., Pan, Q., Yu, W., Chu, Y. (2009). Indium Oxide with Novel Morphology : Synthesis and Application in C_2H_5OH Gas Sensing. Crystal Growth & Design, 9(5), 2146–2151.

[84] Xu, J. Q., Chen, Y. P., Pan, Q. Y., Xiang, Q., Cheng, Z. X., Dong, X. W. (2007). A new route for preparing corundum-type In_2O_3 nanorods used as gas-sensing materials. Nanotechnology, 18(11). https://doi.org/10.1088/0957-4484/18/11/115615

[85] Wang, S., Wang, P., Li, Z., Xiao, C., Xiao, B., Zhao, R., Zhang, M. (2014). Facile fabrication and enhanced gas sensing properties of In_2O_3 nanoparticles. New J. Chem., 38(10), 4879–4884. https://doi.org/10.1039/C4NJ00901K

[86] Yang, H., Yang, Z., Liang, H., Liu, L., Guo, J., Yang, Y. (2010). Solvothermal synthesis of $In(OH)_3$ nanorods and their conversion to In_2O_3. Materials Letters, 64(13), 1418–1420. https://doi.org/10.1016/j.matlet.2010.03.030

[87] Li, Z., Dzenis, Y. (2011). Highly efficient rapid ethanol sensing based on Co-doped In_2O_3 nanowires. Talanta, 85(1), 82–85. https://doi.org/10.1016/j.talanta.2011.03.033

****